



# Zinc Oxide Nanoparticles from Marine Actinomycetes and its Antimicrobial Application

Nisha R.I. <sup>a\*</sup> and Samuel Gnana Prakash Vincent <sup>a</sup>

<sup>a</sup> Centre for Marine Science and Technology (CMST), Manonmaniam Sundaranar University, Rajakkamangalam Kanyakumari District- 629502, Tamil Nadu, India.

## Authors' contributions

*This work was carried out in collaboration between both authors. Both authors read and approved the final manuscript.*

## Article Information

DOI: <https://doi.org/10.56557/upjoz/2024/v45i184475>

## Open Peer Review History:

This journal follows the Advanced Open Peer Review policy. Identity of the Reviewers, Editor(s) and additional Reviewers, peer review comments, different versions of the manuscript, comments of the editors, etc are available here: <https://prh.mbimph.com/review-history/3442>

**Original Research Article**

**Received: 17/06/2024**

**Accepted: 21/08/2024**

**Published: 18/09/2024**

## ABSTRACT

The aim of the study is to biosynthesize and characterize Zinc oxide nanoparticles (ZnO-NPs) and to evaluate their antibacterial potential. Several isolates of the actinomycetes strain were isolated from marine sediments, and the strain was morphologically identified as actinomycetes and screened for ZnO-NPs synthesis. N5 strain showed potent activity while screening against human pathogens and further ZnO-NPs were synthesized for anti-bacterial studies. The ZnO-NPs were characterized using physio-chemical techniques such as ultraviolet spectroscopy, Fourier-Transform Infrared spectroscopy (FTIR), and X-Ray diffraction (XRD). The morphology of ZnO-NPs was analyzed using Scanning Electron Microscopy (SEM) and revealed cubic shaped. The synthesized ZnO-NPs were subjected for their antibacterial potential against human pathogens of both gram-positive and negative bacteria, using the agar well diffusion method. The ZnO-NPs showed positive results on both pathogens, Staphylococcus showed higher activity, followed by E. coli. The synthesized ZnO-NPs have good antibacterial activity which pay way to develop new antimicrobial compounds in pharmaceutical sectors.

\*Corresponding author: Email: [nishabio13@gmail.com](mailto:nishabio13@gmail.com);

**Cite as:** R.I., Nisha, and Samuel Gnana Prakash Vincent. 2024. "Zinc Oxide Nanoparticles from Marine Actinomycetes and Its Antimicrobial Application". *UTTAR PRADESH JOURNAL OF ZOOLOGY* 45 (18):577-87. <https://doi.org/10.56557/upjoz/2024/v45i184475>.

**Keywords:** Zinc oxide; nanoparticles; antimicrobial; actinomycetes; pathogens; marine.

## 1. INTRODUCTION

A wide variety of novel antibiotics can be manufactured with the help of nanotechnology, which offers promising technological tools and appears to have enormous potential in the biomedical and life sciences fields.

It can be categorized into three types: physical, chemical, and biogenic, and it is now causing a lot of interest. Although nanoparticles (NPs) have been produced using all three methods, the chemical and physical processes are associated with high temperatures, high pressures, expensive equipment, and environmental damage [1,2]. Conversely, the synthesis of green nanoparticles is increasingly being done via biological methods [3]. Compared to alternative methods, they have many benefits, such as being hygienic and economical and typically involving one-step protocols [4]. Moreover, the optical, photoelectrical, and chemical properties of NPs generated biologically are some of their most distinctive features, enabling a variety of industrial, medical, and agricultural applications [5, 6, 7, 8]. According to Dhoble and Kulkarni [9] and Zarina and Nanda [10], metal nanoparticles have been effectively produced biologically from a variety of biological sources, most notably microbes. Materials with unique physical, chemical, optical, and electrical properties can be created by the synthesis of nanoparticles using microbial processes. Actinobacteria, in particular, are a significant class of microorganisms that have the potential to be employed in the production of innovative industrial and therapeutic products, including antimicrobials [11]. Many different products with structurally unique and physiologically active metabolites can be found in the marine environment. According to Mohamedi et al. [12], these products may include natural immune stimulants that help ward off infectious illnesses. A class of gram-positive filamentous bacteria known as actinomycetes is frequently found in soil [13]. Due to their ability to degrade soil and their strong antibiotic-producing capacity, these organisms have been extensively researched.

Regarding the biological synthesis of ZnO-NPs, the mechanism has not been thoroughly elucidated. Because of their efficiency, scalability, and capacity to use the entire life cycle of the organism, microbial approaches are

superior to cell culture and the use of plant sources [14]. The microbial production of ZnO nanoparticles from actinomycetes species is the focus of this work. ZnO-NPs are accepted as safe, nontoxic, biocompatible, or GRAS particles. The biological approach is beneficial for synthesizing ZnO-NPs since it is straightforward and maintains antibacterial efficacy. These particles have a wide range of potential antibacterial activity against pathogenic microbes, depending on their age. The biological synthesis of nanoparticles is a viable, cost-effective, and safe synthesis route according to biomedical applications, which confers potential and is more functional. ZnO can also be used in human medicine as an astringent (for wound healing), and to treat hemorrhoids, eczema and excoriation [15]. ZnO nanoparticles have recently attracted attention Owing to their unique features. There are numerous promising applications of ZnO nanoparticles in veterinary Science due to their Wound healing, antibacterial, antineoplastic and antineogenic properties.

## 2. METHODOLOGY

### 2.1 Experiment

Each ingredient employed comes from HiMedia's with AR grade. This comprises zinc sulfate, NaOH, and starch casein agar. The glass components are disinfected and of off-borosil quality.

#### 2.1.1 Isolation of Actinomycetes

A soil specimen was serially diluted with clean distilled water [16] to a concentration of 10<sup>-6</sup> and then plated on starch casein agar plates. Each dilution yielded 0.1 mL, which was then transferred onto plates that contained starch casein nitrate agar media. Until actinomycetes colonies appeared, incubating the plates for 72 hours at 37 °C. According to the investigation, these colonies were intended for future usage and looked dry and powdery.

#### 2.1.2 Morphological Identification

First, the actinomycetes species must be confirmed by morphologically identifying soil isolates. Observations of the colonies on the agar plates are done both macroscopically and

microscopically. The colonies were subjected to macroscopic description using characteristics like mycelial morphology, density, color, shape and size. In addition, spore formation was tracked using the prior report as a guide. At last, significant features were observed under a microscope and identified as actinomycetes.

### 2.1.3 Microbial synthesis of ZnO-NPs

After being inoculated into a broth made of starch, and nitrate, the well-cultured actinomycetes were kept at their normal temperature upto 5 days. For the production of ZnO-NPs, actinomycete 50 ml was taken to a test tube containing 0.1 M zinc sulfate and 0.4 M NaOH. It was then shaken and kept at 40 °C for 15 minutes to generate ZnO-NPs. After heating, it was kept in the oven for up to two minutes and cooled. The production of nanoparticles could be confirmed if the nanoparticle settles down and leaves behind white residues present in the bottom of the flask's. The white precipitate was collected by centrifugation after ten minutes at 3000 rpm; it was washed with distilled water 2 to 3 times. For eight hours, the white pellet was dried at 400 oC in a muffle furnace. According to Mirsha et al [17], ZnO-NPs were therefore generated in a powdered form.



**Fig. 1. Synthesis of ZnO NP from actinomycete APN5 strain**

### 2.1.4 Characterization of ZnO nanoparticles

**UV- Vis spectroscopy:** In order to examine the excitation, biologically produced ZnO-NPs were exposed to UV-visible spectroscopy (Shimadzu, Japan) with a resolution of 1 nm was used to measure it. To verify the reduction in size of nanoparticles, an absorbance spectrum scan between 300 and 500 pm was performed [18, 17].

**FTIR analysis:** ZnO-NP binding efficiency was measured by scanning FTIR. For FTIR investigation, powdered dried ZnO-NPs was utilized directly. The FTIR scan result was recorded using 4 cm<sup>-1</sup> and a frequency range of 400 - 4000 cm<sup>-1</sup>.

**XRD analysis:** The XRD of ZnO-NPs was done with copper K- alpha X-ray energy and having the range of 20 - 80 nm. The appearance, crystal structure, and size of zinc oxide ZnO-NPs were identified by XRD spectroscopy. The dimension of the NPs was found out through Scherrer's equation:

$$D = \frac{K\lambda}{\beta \cos \theta'}$$

It gives the average crystallite dimension and the wavelength and is bragg's angle of X-ray were the same ( $K_g = 0.94$ ).

**Scanning Electron Microscope (SEM):** SEM was used to determine the surface structure of the nanomaterials. ZnO-NPs were dissolved in 100% ethanol while being stirred with an ultrasonic mixer. Part of the solutions were then dropped onto a glass slide, and the solvent was allowed to evaporate at the ambient temperature. SEM analysis, these samples were first covered with a thin coating of copper, about 3 nm in thickness, using physical vapor deposition in a vacuum.

**Antibacterial Assay:** Disk diffusion assays were performed according to Sterile paper disks (5 mm diameter) were prepared using Whatman no. 1 filter paper autoclaved for 15 min at 121 °C and impregnated with 20 µl (500 mg/ml) of the ZnO-NPs [19]. The bacterial strains (*Staphylococcus aureus* and *E. coli*) were sub-cultured in Nutrient agar for 24 hrs prior to use. Test organisms were separately suspended in a 5-ml Nutrient broth. Turbidity was compared using McFarland's solution. The concentration of bacteria in each solution was approximately 1.2 x 10<sup>8</sup>cfu/ml. Mueller-Hinton Agar (MHA) was surface inoculated with this suspension for each organism. The ZnO-NPs were placed on the MHA medium, and the plates were incubated at 32 °C for 24 h. Chloramphenicol (500 mg/ml) was used as a positive control, and water as a negative control. The diameters (mm) of the growth inhibition halos caused by the were measured. The antibacterial assay was carried out in triplicate.

### 3. RESULTS AND DISCUSSION

#### 3.1 Actinomycetes Culture from Soil Isolation

A culture isolation procedure was performed on the obtained soil samples. Following the serial dilution technique, actinomycetes cells were isolated in SCA media (starch casein nitrate agar). The APN5 isolate, which showed white aerial mycelium, was then employed to synthesize ZnO-NPs. According to this, actinomycetes were employed by Rajamanickam et al. [20] to biosynthesize zinc nanoparticles for application in antimicrobial food packaging. Actinomycete-mediated biogenic metal oxide nanoparticles (CuO NPs) have proven to be highly successful previously in combating harmful bacteria and cancer cells [21]. According to Aeruginosa et al. (1982) and Balagurunathan et al. (2011), there is evidence to suggest that green manufactured nanoparticles have a greater inhibitory effect on different kinds of bacteria. As a result, ZnO NPs produced by rare actinomycete were shown to have enhanced antibacterial activity demonstrated by antimicrobial inhibition research, revealing their higher biosource capacity for nanoparticle synthesis [21].

#### 3.2 Microbial Synthesis of Zinc Oxide Nanoparticles

Actinomycetes were cultured on starch casein nitrate broth in order to carry out the microbial production of ZnO-NPs. After one isolate was identified under the microscope, its potential to generate ZnO-NPs was assessed. ZnO-NPs were synthesized, as evidenced by the white precipitate that developed with the isolate. 60 mg of ZnO-NPs were produced by treating the culture extract with zinc sulfate for 96 hours at 37 degrees Celsius. ZnO-NPs were synthesized from ZnSO<sub>4</sub> by actinomycetes.

#### 3.3 Zinc Oxide Nanoparticles

By the support of enzymes and the actinomycete isolates' metabolic processes, the particles were shrunk from micro to nano size. Zinc oxide with a nanoscale has far more capacity than zinc oxide with a micron size. Not all microorganisms can produce NPs since each one has a unique metabolic process and enzyme activity. Mohamed et al. [22] state that the generation of

nanoparticles depends on the selection of the appropriate microorganisms, regardless of their metabolic pathways or level of enzyme activity. Previous studies using microorganisms and plants to synthesize ZnO-NPs revealed absorption peaks in the similar region.

In a similar vein, ZnO NPs were produced by Datta et al. [23] using *Parthenium hysterophorus* leaf extracts. & Ibrahim et al. (2017) used *Aspergillus niger* to create ZnO nanoparticles. Ishra et al. (2013) reported synthesizing ZnO NPs with *Lactobacillus sporangens* and demonstrated the nanoparticle existence by detecting the production of a white powder residue at the flask's bottom. Rajabairavi et al. (2017) used endophytic bacteria *Sphingobacterium thalophilum* to perform the production of zinc oxide nanoparticles in another investigation. Kavitha et al. (2017) used the terpenoid fractions of *Andrographis peniculata* leaves to mediate the synthesis of zinc oxide nanoparticles.

#### 3.4 UV Spectroscopy Analysis

ZnO-NPs were confirmed to be present in the solution by looking at their absorption spectra as seen by the UV visible spectrophotometer. A UV spectrometer was used to first confirm whether or not ZnO-NPs had been detected based on the colloidal nature that was available. The results showed that ZnO-NPs peaks were available between 330 nm and 430 nm. This demonstrates that the sample generated ZnO-NPs. The sample displayed peak values at 330 and 430 nm, respectively (Fig. 3), indicating that ZnO-NPs was the generated. The resultant absorption peak at 364 nm, which was in identifying with the range of ZnO-NPs examination, was comparable to that of the results determined by Mishra et al. [17] and Pandayet al. 2020. Santosh et al. [18] also detected the absorbance peak at 380 nm. From the above studies, we concluded the presence of ZnO -NPs in the biosynthesized samples, a shift in wavelength was observed between 210 nm and 80 nm and there was a gradual decrease. Maximum absorption was observed in the material at 335 nm. Over the past few decades, 3.69 eV results similar to zinc oxide (ZnO) have attracted a lot of attention due to notable characteristics brought about by a large direct band gap of 3.37 eV and a comparatively high exciton binding energy of 60 meV [24].

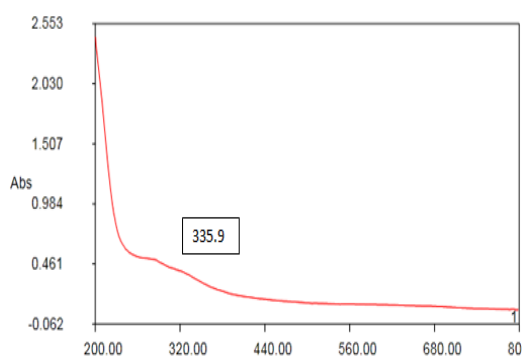


**Fig. 2. Ultraviolet-Visible spectrum of actinomycete APN5 strain showing maximum peak at 335 nm producing ZnO-NPs**

*Lactobacillus plantarum* TA4 cell-free filtrate and bacterial cells were used by Yusof et al. [25] to generate ZnO-NPs; the UV-vis absorption spectrum analysis revealed absorption maxima at 349 and 351 nm, respectively [26]. According to Ghoderao et al. [27], ZnO is generally found to be an n-type semiconductor that slows down the recombination of electron-hole pairs. It has a significant exciton binding energy of 60 meV at ambient temperature and a wide bandgap energy of 3.37 eV reported by Shidpour et al. [28].

### 3.5 FTIR Analysis

FTIR data would provide definitive information on the presence or absence of different modes of vibration in produced ZnO NPs. It is already established because the surface area to volume ratio for the nanoparticle is larger compared with their bulk counterparts.

The ZnO-NPs have FTIR spectra between 4000 and 400  $\text{cm}^{-1}$ . At 3943.67  $\text{cm}^{-1}$ , 3843.29  $\text{cm}^{-1}$ , and 3209.07  $\text{cm}^{-1}$ , the widened appearance of powerful bands with the O-H bond group was confirmed.

The OH peaks indicate the presence of residual moisture irrespective of the heating and drying of samples. The peak bands at 1628.584  $\text{cm}^{-1}$ , 1618.55  $\text{cm}^{-1}$ , 1528.84  $\text{cm}^{-1}$ , 1344.60  $\text{cm}^{-1}$  represent C = O stretching of COO and CHO moiety and C-O stretching was confirmed at 1095  $\text{cm}^{-1}$ , 446.90  $\text{cm}^{-1}$ , and 416.08  $\text{cm}^{-1}$  of the bonds were confirmed zinc oxide bonds. The samples Shows prominent peaks at 3943.67  $\text{cm}^{-1}$ , 3843.29  $\text{cm}^{-1}$ , 3209.07  $\text{cm}^{-1}$ , 2909.16  $\text{cm}^{-1}$ , 2925.15  $\text{cm}^{-1}$ , 2856.08  $\text{cm}^{-1}$ , 1740.22  $\text{cm}^{-1}$ , 1651.89  $\text{cm}^{-1}$ , 1628.584  $\text{cm}^{-1}$ , 1618.55  $\text{cm}^{-1}$ , 1528.84  $\text{cm}^{-1}$ , 1344.60  $\text{cm}^{-1}$ , 1234.72  $\text{cm}^{-1}$ , 1151.32  $\text{cm}^{-1}$ ,

1184.10  $\text{cm}^{-1}$ , 823.13  $\text{cm}^{-1}$ , 692.43  $\text{cm}^{-1}$ , 601.74  $\text{cm}^{-1}$ , 446.90  $\text{cm}^{-1}$ , and 416.08  $\text{cm}^{-1}$  respectively.

The generation of ZnO-NPs is confirmed by the FTIR data. Similar findings have been observed with ZnO-NPs at 424  $\text{cm}^{-1}$  and 462.25  $\text{cm}^{-1}$ . The ZnO-NPS generated with the green technique, as reported by Al-Dabhi et al [16], had a strongest peak at 417  $\text{cm}^{-1}$ . The ZnO-NPS, which was made by using the leaves of plants extract, contains peaks in the wavelength range of 500 - 4000  $\text{cm}^{-1}$ . Baliah et al. [29] found that the ZnO- NPs made with extract of onion pulp, maximum peak between 3421  $\text{cm}^{-1}$  and 677  $\text{cm}^{-1}$ .

The extracellular enzymes secreted into the growth media or present on the microbial cell membrane could be involved in the formation of nanoparticles through protein molecules, primarily by reducing enzymes. The synthesis that occurs without the use of enzymes is dependent on specific organic functional groups found on the cells of microbial wall. These groups aid in the reduction of metal ions, as reported by Mohamed et al. in 2019. According to Kapoor et al. [30], there were protein and amide I and II bands found in our sample. These bands could potentially play a part in the establishment and sealing of the metals. Furthermore, Tiwari et al. [31] reported that the metal oxides exhibited peak absorption values of less than 1200  $\text{cm}^{-1}$ , which were attributed to interatomic vibrations and denoted the ZnO-NPs' fingerprint zone.

### 3.6 XRD Analysis

A more thorough understanding of a nanoparticle's crystallinity can be gained from XRD spectra. The broader spectrum of the typical XRD spectra is frequently associated with the production of crystalline ZnO-NPs. XRD spectroscopy was used to assess the ZnO-NPs that were extracted from the APN5 sample in order to investigate their crystalline nature. (Fig. 5).

Based on data from the Joint Committee on Powder Diffraction Standards (JCPDS card number 36-1451), all of the XRD peak values in all of the observed patterns could be indexed to monophasic zinc oxide hexagonal wurtzite structure. The ZnO-NPs were identified as having a particle size of  $2\theta = 33.42^\circ$  18.05 nm, respectively.

<https://instanano.com/all/charecterization/xrd/>

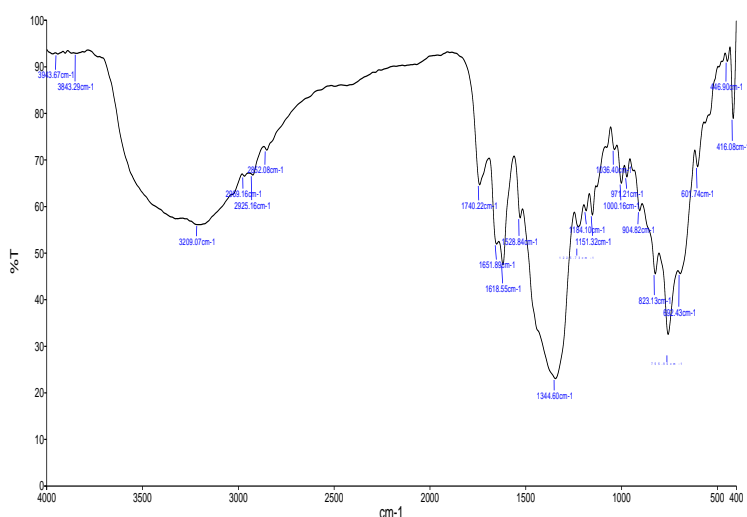


**Fig. 3. FTIR Spectrum of actinomycete APN5 strain presents in ZnO-NPs**

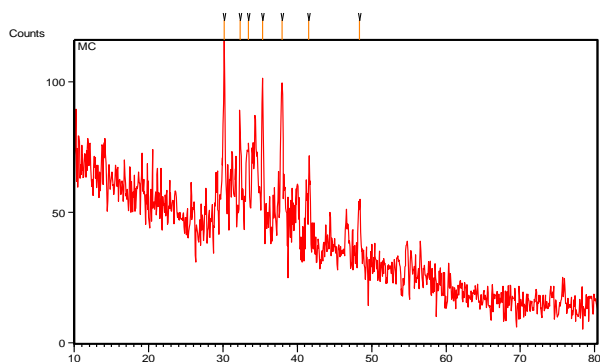


**Fig. 4. The XRD pattern of actinomycete APN5 strain the broad reflection seen at  $2\theta = 33.42^\circ$  shows Zinc oxide ZnO- NPs present in actinomycetes**

crystallite-size/ XRD crystallite (grain) Size Calculator (Scherrer Equation) – Insta Nano (retrieved August 16, 2024). According to Insta Nano's XRD d value calculator (<https://instanano.com/all/characterization/xrd/d-value/accesses> August 14, 2024), the XRD d value is 0.27 nm. The spectral length of an X-ray ranges from 0.01 and 10 nm. when a result, X-rays may easily enter the crystal structure of any material and reveal information about its qualities when they exit it. This is the reason why X-ray spectroscopy is a highly helpful technology for characterizing various kinds of materials. XRD analysis of the ZnO-NPs that were created by a green method reported by Al dabhi et al. [16]. On the other hand, Kalilh et al. (2014) used the Debye-Scherrer equation for analysis, obtaining the highest intensity peak at  $2\theta$  (36.67o). File 043-0002 is the standard JCPDS pattern for ZnO. Consequently, a prominent peak in the XRD result pattern revealed the organized

crystalline framework of ZnO-NPs. The crystalline structure and lattice of the nanoparticle were identified with the use of XRD.

### 3.7 SEM Analysis

The size, form, and structure of ZnO-NPs obtained from APN5 are explained by the SEM technique. The SEM picture shows how much potential actinomycetes have to create distinct, needle-shaped ZnO-NPs. Two magnifications (10,000 and 100,000) were used to view SEM images. The produced ZnO-NPs' SEM pictures revealed needle like crystals structures with a standard particle dimension of 321.3 nm (Fig. 6). Shanmuga Sundaram and Balagurunathan [32] found that the SEM study of ZnO-NPs produced from *Streptomyces* species revealed a spherical form with a standard particle size of 16–25 nm. On the other hand, zinc oxide produced by *S. thalophilum* exhibited a similarly sized triangular

structure, with an average size of 112 nm. Santhosh et al.'s confirmation of ZnO-NPs' spherical shape is encouraging (2017). Additionally, 1µm-diameter cuboids shaped ZnO-NPs were discovered in this investigation.

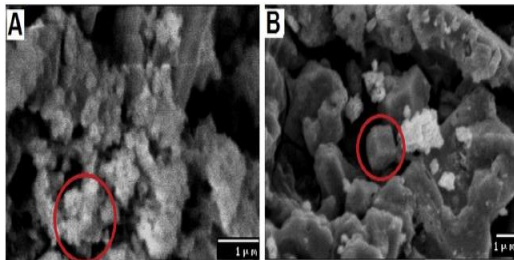


**Fig. 5. Cubic shape Zinc oxide ZnONPsactinomyceteAPN5 strain (A) ZnONPs visible a cauliflower shape. (B) Nanoparticles with great consistency.**

### 3.8 Antibacterial Assay for Well Diffusion Method

Two different human pathogenic bacterial strains were selected for the study. The synthesized ZnO-NPs showed an inhibition zone of 14 mm and 12 mm against *Staphylococcus aureus* and *Escherichia coli*, respectively.

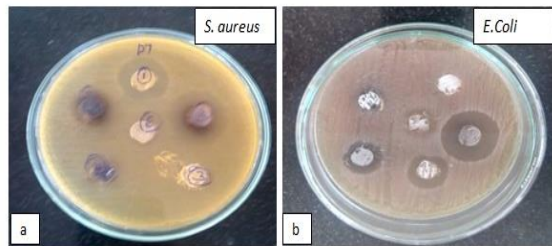


**Fig. 6. Antibacterial activity of microbial synthesized ZnO-NPs Actinomycete APN5 strain against human pathogens *Staphylococcus aureus* and *E. coli***

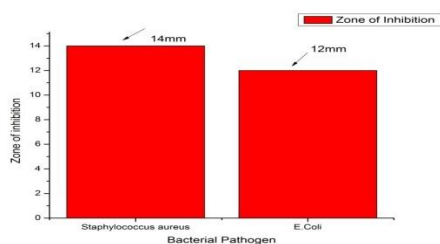


**Fig. 7. Relative study of antimicrobial effect of actinomycete APN5 strain**

At higher concentrations, the biosynthesized ZnO-NPs were reported to exhibit antibacterial efficacy against microorganisms that were resistant to multiple drugs. An efficient zone of inhibition was seen against *Enterococcus* sp., *Staphylococcus aureus*, and *Proteus mirabilis*, while ZnO-NPs shown increased antibacterial action against resistant bacteria [33]. However, it was discovered that the synthesis of ZnO-NPs by marine yeast had potent antibacterial action against the human diseases *B. subtilis* and *E. coli*. At a dose of 100 µg/mL, the well-diffusion test revealed a wider inhibitory zone against *B. subtilis* and *E. coli*. But because Gram-positive and negative bacteria have distinct cell wall compositions, ZnO-NPs' antibacterial activity against *E. coli* was more effective than it was against *B. subtilis* [34]. Using stevia leaves, a green synthesis method produces rectangular ZnO-NPs with strong bactericidal action against *E. coli* and *S. aureus*. The results, as reported by Khatami et al. [35], showed that the MIC value of the R-ZnO-NPs reached 2.0 µg/mL while they exhibited a greater antibacterial effect at smaller doses. In an investigation evaluating the antibacterial impacts of the two, ZnO-NPs have been shown to have stronger toxicity impacts on *B. subtilis*, *E. coli*, and *P. fluorescens* compared to their bulk particle equivalents.. The counterparts showed no toxicity or reduced toxicity. This suggests that toxicity is affected by particle size [36]. After 8 hours of incubation, At an NP concentration of 0.0025 mg ml<sup>-1</sup>, the ZnO NPs demonstrated strong antibacterial activity against *Escherichia coli*, *Staphylococcus aureus* in without the use of UV radiation. Specifically, the synthesis parameters had a significant impact on the bactericidal ability against *S. aureus*.

The process included the movement of efficient Zn<sup>+</sup> ion molecules, which made it simple for the ZnO NPs to readily degrade the negative charges on the bacterial surface (caused by the existence of charged phosphate and carboxyl residues on their the outermost membrane). By ZnO NPs, on the other hand, have a charge that is positive. Following then, Praveena et al [37] reported that, there was damage to the bacterial cell wall and total distraction of the porin channels. Subsequently, it impacted the lipid bilayer and teichoic acid within the bacterial cells. After joining the bacterial porin channels, the Zn<sup>+</sup> ions lost their antigenicity [38]. Eventually, the ZnO-NPs treated cells' depletion of vital components was killed, and they continued to be in the decline phase. The obtained anti-biofilm

and severely damaged internal and extracellular bacterial components, based on the mechanism described above [39-42].

#### 4. CONCLUSION

The ultraviolet-visible spectrum of actinomycete APN5 strains shows a maximum peak at 335 nm, producing ZnO-NPs. The XRD pattern of actinomycete APN5 strain, the broad reflection seen at  $2\theta = 36.67^\circ$ , shows Zinc oxide ZnO-NPs present in actinomycetes. The images from scanning electron microscopy showed that the ZnO-NPs from the actinomycete APN5 strain were cubic in nature (A) picture represented ZnO-NPs looks similar to cauliflower (B) this image showed the cubic NPs have great consistency. With all the above results obtained from this study, we conclude that the soil sample APN5 strain have a rich source of secondary metabolites that inhibit bacterial pathogens. The synthesized ZnO-NPs is an efficient green synthesis route, having good antibacterial activity possessing an extensive array of possible uses, particularly in the biomedical industry, and may be employed in the creation of novel antibiotics.

#### ACKNOWLEDGEMENT

I thank all members of cmst and ms university tirunelveli for support in this work and for valuable suggestions.

#### DISCLAIMER (ARTIFICIAL INTELLIGENCE)

Author(s) hereby declare that NO generative AI technologies such as Large Language Models (ChatGPT, COPILOT, etc) and text-to-image generators have been used during writing or editing of this manuscript.

#### COMPETING INTERESTS

Authors have declared that no competing interests exist.

#### REFERENCES

1. Taner M, Sayar N, Yulug IG, Suzer S. Synthesis, characterization and antibacterial investigation of silver–copper nanoalloys. *Journal of Materials Chemistry*. 2011;21(35):13150-13154. DOI:10.1039/C1JM11718A
2. Wang C, Kim YJ, Singh P, Mathiyalagan R, Jin Y, Yang DC. Green synthesis of silver nanoparticles by *Bacillus methylophilicus*, and their antimicrobial activity. *Artificial Cells, Nanomedicine, and Biotechnology*. 2016;44(4):1127-1132. DOI: 10.3109/21691401.2015.1011805
3. Pandey S, De Klerk C, Kim J, Kang M, Fosso-Kankeu E. Eco-friendly approach for synthesis, characterization and biological activities of milk protein stabilized silver nanoparticles. *Polymers*. 2020;12(6):1418. DOI:10.3390/polym12061418
4. Pandey S, Ramontja J. Sodium alginate stabilized silver nanoparticles-silica nanohybrid and their antibacterial characteristics. *International Journal of Biological Macromolecules*. 2016;93:712–723. DOI:10.1016/j.ijbiomac.2016.09.033
5. Barani M, Mukhtar M, Rahdar A, Sargazi S, Pandey S, Kang M. Recent advances in nanotechnology-based diagnosis and treatments of human osteosarcoma. *Biosensors*. 2021;11(2):55. DOI: 10.3390/bios11020055
6. Sabir F, Zeeshan M, Laraib U, Barani M, Rahdar A, Cucchiarini M, Pandey S. DNA based and stimuli-responsive smart nanocarrier for diagnosis and treatment of cancer: applications and challenges. *Cancers*. 2021;13(14):3396. DOI: 10.3390/cancers13143396
7. Ojo SA, Lateef A, Azeez MA, Oladejo SM, Akinwale AS, Asafa TB, Yekeen TA, Akinboro A, Oladipo IC, Gueguim-Kana EB, Beukes LS. Biomedical and catalytic applications of gold and silver-gold alloy nanoparticles biosynthesized using cell-free extract of *Bacillus safensis* LAU13: Antifungal, dye degradation, anti-coagulant and thrombolytic activities. *IEEE Trans. Nano bioscience*. 2016;15(5):433-442. DOI:10.1109/TNB.2016.2559161
8. Couto EAA, Dias-Arieira CR, Kath J, Juliana AH, Puerari HH. Boron and zinc inhibit embryonic development, hatching and reproduction of *Meloidogyne incognita*, *Acta Agriculturae Scandinavica. Section B-Soil & Plant Science*. 2016;66(4):346–352. DOI:10.1080/09064710.2015.1118154
9. Dhoble SM, Kulkarni NS. Biosynthesis and Characterization of Different Metal Nanoparticles by Using Fungi. *Scholars Academic Journal of Biosciences*. 2016;4:1022–1031.



10. Zarina A, Nanda A. Combined Efficacy of Antibiotics and Biosynthesised Silver Nanoparticles from *Streptomyces Albaduncus*. International Journal of Pharmaceutical Research & Technology. 2014;6(6):1862–1
11. Bhosale RS, Hajare KY, Mulay B, Mujumdar S, Kothawade M. Biosynthesis, characterization and study of antimicrobial effect of silver nanoparticles by *actinomycetes* spp. International Journal of Current Microbiology and Applied Sciences. 2015;2:144–151.
12. Mohamedin A, El-Naggar NEA, Shawqi Hamza S, Sherief AA. Green synthesis, characterization and antimicrobial activities of silver nanoparticles by *Streptomyces viridodiastaticus* SSHH-1 as a living nanofactory: statistical optimization of process variables. Current Nanoscience. 2015;11:640-654. DOI:10.2174/1573413711666150309233939
13. Prudence SMM, Addington E, Castaño-Espriu L, Mark RD, Pintor-Escobar L, McLean TC. Advances in actinomycete research: An actinobase review of 2019. Microbiology Society (United Kingdom). 2020;166:683–694. Available:https://doi.org/10.1099/mic.0.000944
14. MohdYusof H, Mohamad R, Zaidan UH, Abdul Rahman NA. Microbial synthesis of zinc oxide nanoparticles and their potential application as an antimicrobial agent and a feed supplement in animal industry. A review. Journal of Animal Science and Biotechnology. 2019;10:1–22. Available:https://doi.org/10.1186/s40104-019-0368-z
15. Ozgur U, Hofstetter D, Morkoc H, Proc. IEEE. 2010;98(7):1255–1268
16. Al-Dhabi N, ValanArasu M. Environmentally friendly green approach for the production of zinc oxide nanoparticles and their anti-fungal, ovicidal, and larvicidal properties. Nanomaterials. 2018;8(7):500. Available:https://doi.org/10.3390/nano8070500
17. Mishra M, Paliwal JS, Singh SK, Selvarajan E, Subathradevi C, Mohanasrinivasan V. Studies on the inhibitory activity of biologically synthesized and characterized zinc oxide nanoparticles using *lactobacillus sporogens* against *staphylococcus aureus*. Journal of Pure and Applied Microbiology. 2013;7(2);1263-1268.
18. Santhosh kumar J, Kumar SV, Rajeshkumar S. Synthesis of zinc oxide nanoparticles using plant leaf extract against urinary tract infection pathogen. Resour. Technol. 2017;3(4):459-465. Available:https://doi.org/10.1016/j.reffit.2017.05.001.
19. Ruangpan L, Tendencia EA. Laboratory manual of standardized methods for antimicrobial sensitivity tests for bacteria isolated from aquatic animals. Southeast Asian Fisheries Development Center (SEAFDEC). 2004;37(2), 13-27.
20. Rajamanickam U, Viswanathan S, Muthusamy P. Biosynthesis of zinc nanoparticles using actinomycetes for antibacterial food packaging. International Conference on Nutrition Food Science. 2012;39:195-199.
21. Golinska P, Wypij M, Ingle AP, Gupta I, Dahm H, Rai M. Biogenic synthesis of metal nanoparticles from actinomycetes: biomedical applications and cytotoxicity. Applied Microbiology and Biotechnology. 2014;98:8083- 8097. DOI: 10.1007/s00253-014-5953-7
22. Mohamed Yusof H, Mohamad R, Zaidan UH, Abdul Rahman NA. Microbial synthesis of zinc oxide nanoparticles and their potential application as an antimicrobial agent and a feed supplement in animal industry A Review. Journal of Animal Science and Biotechnology. 2019;10(57):1-22. Available:https://doi.org/10.1186/s40104-019-0368-z
23. Datta A, Patra C, Bharadwaj H, Kaur S, Dimri N, Khajuria R. Green synthesis of zinc oxide nanoparticles using *Partheniumhysterophorus* leaf extract and evaluation of their antibacterial properties. Journal of Biotechnology & Biomaterials. 2017;271. DOI:10.4172/2155-952X.1000271
24. Andrade GR, Nascimento CC, Lima ZM, Teixeira-Neto E, Costa LP, Gimenez IF. Star-shaped ZnO/Ag hybrid nanostructures for enhanced photocatalysis and antibacterial activity. Appl Surf Sci. 2017;399:573–582.
25. Yusof HM, Mohamad R, Zaidan UH, Samsudin AA. Biosynthesis of zinc oxide nanoparticles by cell-biomass and supernatant of *lactobacillus plantarum* ta4 and its antibacterial and biocompatibility

- properties, *Scientific Reports*. 2020;10(1): 19996.  
DOI: 10.1038/s41598-020-76402-w.
26. Ehsan S, Sajjad M. Bioinspired synthesis of zinc oxide nanoparticle and its combined efficacy with different antibiotics against multidrug-resistant bacteria, *Journal of Biomaterials and Nanobiotechnology*. 2017;8(2):159-175.  
DOI:10.4236/jbnb.2017.82011
  27. Ghoderao KP, Jamble SN, Kale RB. Influence of pH on hydrothermally derived ZnO nanostructures. *Optik*. 2018;156, 758-771.
  28. Shidpour R, Simchi A, Ghanbari F, Vossoughi M. Photo-degradation of organic dye by zinc oxide nanosystems with special defect structure: Effect of the morphology and annealing temperature. *Applied Catalysis A: General*. 2014;472:198-204.
  29. Baliah NT, Muthulaksmi P, Priyatharsini SL. Synthesis and characterization of onion mediated silver doped zinc oxide nanoparticles, *International Journal of Scientific Research in Science, Engineering and Technology*. 2018;4:111-120.  
Available:<https://doi.org/10.32628/ijsrset11841129>
  30. Kapoor RT, Salvadori MR, Rafatullah M, Siddiqui MR, Khan MA, Alshareef SA. Exploration of microbial factories for synthesis of nanoparticles- a sustainable approach for bioremediation of environmental contaminants, *Frontiers in Microbiology*. 2021;12  
Available:<https://doi.org/10.3389/fmicb.2021.658294>
  31. Tiwari V, Mishra N, Gadani K, Solanki PS, Tiwari M. Mechanism of Anti-bacterial activity of Zinc Oxide nanoparticle against Carbapenem-resistant, *Acinetobacterbaumannii*, *Frontiers in Microbiology*. 2018;9.  
Available:<https://doi.org/10.3389/fmicb.2018.01218>
  32. Shanmuga Sundaram T, Balagurunathan R. Bio-medically active zinc oxide nanoparticles synthesized by using extremophilic *actinobacterium*, *Streptomyces* sp. (MA30) and its characterization, *Artificial Cells, Nanomedicine, and Biotechnology*. 2017; 45(8):1521–1529.  
Available:<https://doi.org/10.1080/21691401.2016.1260577>.
  33. Chauhan R, Reddy A, Abraham J. Biosynthesis of silver and zinc oxide nanoparticles using *Pichiafermentans* JA2 and their antimicrobial property. *Applied Nanoscience*. 2015;5:63-71.  
DOI 10.1007/s13204-014-0292-7
  34. Balraj B, Senthilkumar N, Siva C. Krithikadevi R, Julie A, Vetha I, Potheher, Arulmozhi M. Synthesis and characterization of zinc oxide nanoparticles using marine *Streptomyces* sp. with its investigations on anticancer and antibacterial activity. *Research on Chemical Intermediates*, 2017;43(4):2367-76.  
DOI:10.1007/s11164-016-2766-6
  35. Khatami M, Alijani HQ, Heli H, Sharifi I. Rectangular shaped zinc oxide nanoparticles: green synthesis by stevia and its biomedical efficiency. *Ceramics International*. 2018;44(13):15596-602.  
DOI:10.1016/j.ceramint.2018.05.224
  36. Jiang W, Mashayekhi H, Xing B. Bacterial toxicity comparison between nano- and micro-scaled oxide particles. *Environmental Pollution*. 2009;157(5):1619-25. DOI: 1016/j.envpol.2008.12.025
  37. Praveena V, Venkatalakshmi S, Alharbi NS, Kadaikunnan S, khaled JM, Govindarajan M. Identification of a novel antibacterial protein from hemolymph of freshwater zooplankton. *Mesocyclopsleuckarti*. *Saudi Journal of Biological Science*. 2020;2(9):2390–2397.  
Available:<https://doi.org/10.1016/j.sjbs.2020.05.01>
  38. Vinotha V, Iswarya A, Thaya R, Govindarajan M, Alharbi NS, Kadaikunnan S, Khaled JM, Al-Anbr MN, Vaseeharan B. Synthesis of ZnO nanoparticles using insulin-rich leaf extract: Anti-diabetic, antibiofilm and anti-oxidant properties. *Journal of Photochemistry and Photobiology B: Biology*. 2019;197 111541.  
Available:<https://doi.org/10.1016/j.jphotobiol.2019.111541>
  39. Iwuoha E, Michiralet al. Greenroute synthesis and characterization of ZnO nanoparticles using *Spathodeacampanulata*. *Int. J. Biochem*. 2015;23:53-61.
  40. Brahem EJ, Thalij KM, Saleh MK, Badawy AS. Biosynthesis of zinc oxide nanoparticles and assay of antibacterial activity. *American Journal of Biochemistry and Biotechnology*. 2017;13(2):63-69.  
Available:<https://doi.org/10.3844/ajbbbsp.2017.63.69>.

41. Pandey S, Do JY, Kim J, Kang M. Fast and highly efficient catalytic degradation of dyes using κ-carrageenan stabilized silver nanoparticles Carbohydrate Polymers. 2020;230: 115597.  
DOI:10.1016/j.carbpol.2019.115597
42. Khalil MI, Al-Qunaibit MM, Al-zahem AM, Labis JP. Synthesis and characterization of ZnO nanoparticles by thermal decomposition of a curcumin zinc complex, Arabian Journal of Chemistry. 2014;7(6): 1178–1184.  
Available: <https://doi.org/10.1016/j.arabjc.2013.10.025>.

**Disclaimer/Publisher's Note:** The statements, opinions and data contained in all publications are solely those of the individual author(s) and contributor(s) and not of the publisher and/or the editor(s). This publisher and/or the editor(s) disclaim responsibility for any injury to people or property resulting from any ideas, methods, instructions or products referred to in the content.

© Copyright (2024): Author(s). The licensee is the journal publisher. This is an Open Access article distributed under the terms of the Creative Commons Attribution License (<http://creativecommons.org/licenses/by/4.0>), which permits unrestricted use, distribution, and reproduction in any medium, provided the original work is properly cited.

*Peer-review history:*

*The peer review history for this paper can be accessed here:*

<https://prh.mbimph.com/review-history/3442>